J Neuropathol Exp Neurol
Vol. 79, No. 10, October 2020, pp. 1130–1133
doi: 10.1093/jnen/nlaa066

LETTER TO THE EDITOR

Spinal Cord and Motor Neuron TDP-43 Pathology in a Sporadic Inclusion Body Myositis Patient

Sahara J. Cathcart, MD, Ericka P. Greene, MD, Suzanne Z. Powell, MD, Anithachristy S. Arumanayagam, PhD, Andreana L. Rivera, MD, Rabi Tawil, MD, Stanley H. Appel, MD, and Matthew D. Cykowski, MD

Department of Pathology and Genomic Medicine (SJC, SZP, ASA, ALR, MDC); Stanley H. Appel Department of Neurology (EPG, SHA, MDC); Institute of Academic Medicine at the Houston Methodist Research Institute (EPG, SHA, MDC); Houston Methodist Neurological Institute, Houston, Texas (EPG, SZP, ALR, SHA); and Neuromuscular Disease Unit, Department of Neurology, University of Rochester Medical Center, Rochester, New York (RT)

Send correspondence to: Matthew D. Cykowski, MD, Houston Methodist Hospital, 6565 Fannin Street, Houston, TX 77030. E-mail: mdcykowski@houstonmethodist.org

This study was supported in part by a Clinician-Scientist Recruitment and Retention Program Award from the Houston Methodist Research Institute and an Investigator-Initiated Research Award from the ALS Association (ALSA) (both to MDC).

The authors have no duality or conflicts of interest to declare.

To the Editor:

Inclusion body myositis (IBM) is characterized clinically by weakness, muscle atrophy, and dysphagia (1) and pathologically by inflammation, vacuolar degeneration, and accumulation of misfolded proteins (e.g. p62, TAR DNA-binding protein 43 kDa [TDP-43]) (2). Clinical and electromyographic findings suggestive of a neurogenic component have been reported (3, 4), and multisystem proteinopathies (e.g. with *VCP* mutations) further suggest that IBM can exist with comorbid central nervous system (CNS) pathology (5). In sporadic IBM (sIBM), there is little or no information regarding comorbid CNS pathology.

To address this question, we performed an autopsy with a comprehensive neuropathology examination on an sIBM patient. The patient had a 17-year disease course beginning with proximal arm weakness, facial weakness, and muscle atrophy. EMG studies at presentation suggested a myopathy affecting the face, shoulder girdle, and proximal arm and leg musculature. Facioscapulohumeral muscular dystrophy (FSHD) was initially suspected, but *FSHD1* and *FSHD2* testing was normal. Initial muscle biopsy was nondiagnostic, and the patient showed no improvement on steroids, IVIG, and methotrexate. The patient continued to progress, eventually developing respiratory insufficiency, dysphagia, and finger flexor weakness. Ten years after initial symptoms, repeat muscle biopsy showed an inflammatory myopathy with rimmed vacuoles and membranous whorls on electron microscopy. IBM was diagnosed and subsequent serology studies revealed anticytosolic 5′-nucleotidase 1A autoantibodies. Late in his clinical course, the patient had atrophy and scalloping of the tongue without fibrillations, atrophy of intrinsic hand muscles, deltoids, biceps, calves, and hip flexors, as well as diffuse muscle weakness, decreased tone, and diffusely decreased reflexes. Neuropsychological evaluation revealed no cognitive impairment. Neuromuscular specialists at multiple institutions evaluated the patientand amyotrophic lateral sclerosis (ALS) was not suspected at any time. An autopsy for diagnostic and research purposes was requested after the patient died at age 61 years.

At autopsy, there was significant muscle atrophy, especially of anterior tibialis and gastrocnemius. Formalin-fixed, paraffin-embedded tissue was available for all brain regions, the entirely submitted spinal cord and attached nerve roots, and select muscle groups. Spinal cord sections were stained with hematoxylin and eosin (H&E), N-terminal TDP-43 (10782-2-AP, 1:1000, Proteintech, Chicago, IL), phosphorylated TDP-43 (22309-1-AP, 1:500, Proteintech) and p62 (610833, 1:100, BD Biosciences, Franklin Lakes, NJ) and select sections were stained with FUS (11570-1-AP, Proteintech), LC3 (LC3-5F10, 1:100, Nano Tools, Teningen, Germany), and α-synuclein (32-8100, 1:100, Invitrogen, Carlsbad, CA). Cervical, thoracic, lumbar, and sacral spinal cord levels from patients with ALS ($n = 9$; mean age = 64.1 years) and without either ALS or IBM ($n = 22$; mean age = 63.2 years) were also examined for H&E and TDP-43 pathologies. For the sIBM patient, brain sections were stained with H&E, TDP-43 (10782-2-AP, 1:200, Proteintech), β-amyloid (clone 6F/3D, 1:20, Dako, Glostrup, Denmark), tau

TABLE 1. Next-Generation Sequencing Panel

	High-Risk Genes	Additional Genes
Genes analyzed	*BAG3, FLNC, FUS, FYCO1, HNRNPA1, HNRNPA2B1, SQSTM1, TARDBP, VCP, ZASP*	*ACTA1, CASQ1, CPT2, DNAJB6, DNM2, DPM3, DYSF, FHL1, GLI3, GNE, KLHL41, MATR3, MYF6, MYH2, MYOT, PNPLA2, RYR1, TCAP, TIA1, TNPO3, VMA21*

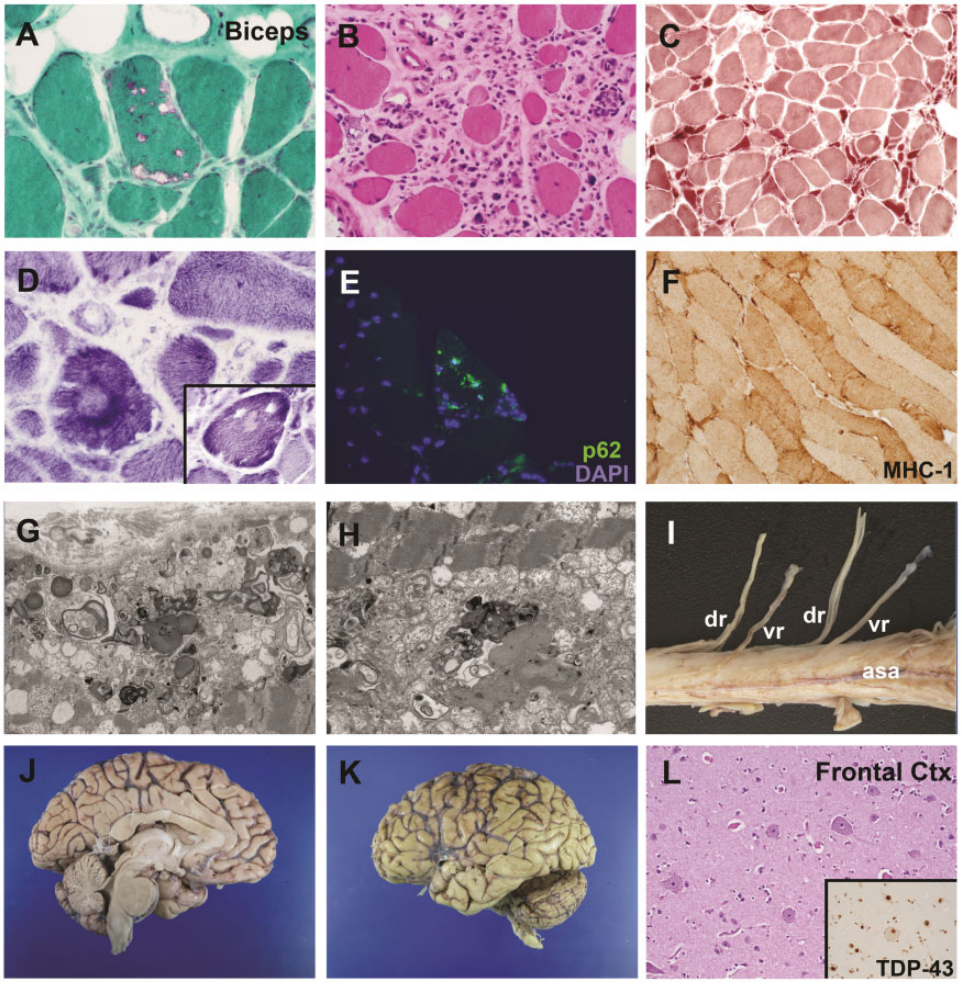

FIGURE 1. Postmortem muscle, spinal cord and brain pathology in sIBM. Postmortem biceps muscle sample with frequent rimmed vacuoles on Gomori trichrome (600× magnification) (**A**) and numerous small, atrophic fibers on H&E (400×) (**B**) and NSE (200x) (**C**). (**D**) Oxidative enzyme stain (NADH) showed rare targetoid fibers (600×). (**E**) Characteristic of sIBM, p62 immunofluorescence was positive for cytoplasmic inclusions (600×) and (**F**) MHC-1 was overexpressed (200×). (**G, H**) Electron microscopy showed membranous whorls and debris (**G, H**) and granulofilamentous material (not shown) characteristic of IBM. (**I**) Photograph of the lumbosacral spinal cord showing atrophic ventral nerve roots (vr) and normal-appearing dorsal roots (dr) (asa, anterior spinal artery). (**J, L**) Medial and lateral views of hemisphere and H&E of agranular frontal cortex (**L**) (200×) appear completely normal and TDP-43 is negative for inclusions in frontal cortex (400×) (inset).

(1:40 000, Dako), α-synuclein (LB209, 1:25, Invitrogen), and p62 (1:1000, BD Biosciences). Muscle samples of diaphragm, deltoid, quadriceps, biceps, paraspinous, and gastrocnemius in the patient were examined, and the biceps sample was processed for the full histochemical muscle panel and electron microscopy. Frozen muscle was submitted for a next-generation sequencing panel of 31 genes implicated in IBM, vacuolar myopathies, and ALS (Table 1).

The postmortem biceps sample showed conspicuous rimmed vacuoles, increased MHC-1 expression, cytoplasmic p62 aggregates, targetoid fibers, and membranous whorls and granulofilamentous inclusions by electron microscopy. Nu-

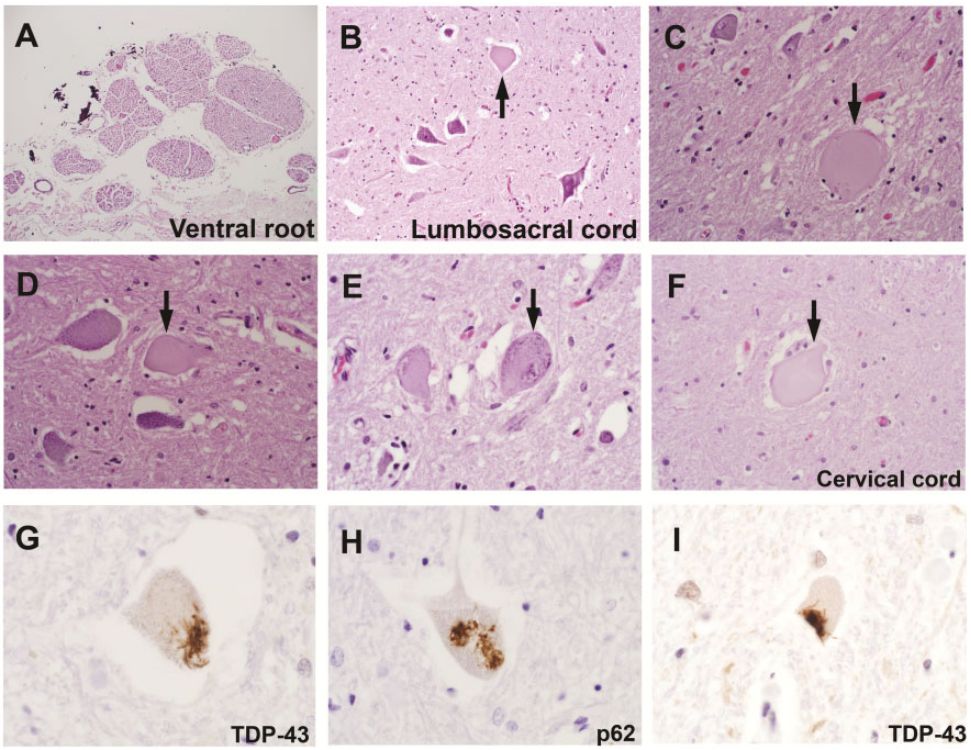

FIGURE 2. Motor neuron and spinal cord pathology in sIBM. (**A**) Ventral root atrophy is seen, corresponding to nerve root atrophy identified on gross examination. (**B–F**) H&E-stained sections show mild neuron loss and gliosis (**B**), as well as enlarged chromatolytic neurons (**B–F**) with markedly swollen cytoplasm, pallor, and dispersion of Nissl substance (black arrows). In lumbosacral cord, sparse skein-like inclusions were identified by TDP-43 (**G, I**) and p62 (**H**) immunostains. (**C–I**) are photographed at 600×, panel **B** at 200×, and panel **A** at 40×.

merous atrophic fibers present and were highlighted by NSE staining (Fig. 1). Within the spinal cord, there was diffuse atrophy of the ventral nerve roots with decreased caliber and gray discoloration, particularly in comparison to normal-appearing dorsal nerve roots (Figs. 1 and 2). Histopathologic evaluation demonstrated mild motor neuron loss with microglial activation and reactive astrogliosis at multiple levels. Scattered chromatolytic neurons were seen in the ventral horn at multiple levels. These cells had pale, markedly enlarged cell bodies with dispersed Nissl substance (Fig. 2). No Bunina bodies were identified, and there was no appreciable tract degeneration. Rare motor neurons had p62, pTDP-43, and N-terminal TDP-43-positive inclusions on successive levels (Fig. 2) and several had a thread or skein-like morphology. FUS and LC3 were negative. The comparison samples (ALS and controls) showed similar motor neuron TDP-43 only in the ALS samples where the pathology was more frequent. A single control sample had rare chromatolytic neurons (H&E), less striking than in the sIBM case and limited to lumbar cord (TDP-43-negative). Primary motor cortex and brainstem motor nuclei were normal and were negative for TDP-43 pathology in the sIBM patient. Incidental Lewy-body disease, brainstem predominant, was identified, including scattered Lewy bodies in the intermediolateral cell column (α-synuclein-positive, pTDP-43-negative). No p62-positive, TDP-43-negative inclusions were identified in granular neurons of the dentate gyrus or cerebellum, excluding *C9ORF72* expansion, and no sequence variants were identified in *FUS*, *SQSTM1*, *TARDBP*, or *VCP*, among other genes (Table 1).

To our knowledge, this is the first study with a detailed description of spinal cord pathology in sIBM, including ventral nerve root atrophy, chromatolytic neurons, and rare motor neurons with p62 and pTDP-43 inclusions. This report adds sIBM to the list of non-ALS entities with motor neuron TDP-43 inclusions—a list that includes facial-onset sensory and motor neuronopathy (6), paraneoplastic lower motor neuron disease with sensorimotor neuropathy (7), hereditary spastic paraplegia 6 (SPG6) (8), and Machado-Joseph disease (9). The H&E and pTDP-43 pathology in the sIBM spinal cord were milder than in ALS spinal cords, even in cases with mild ALS pathology. No Bunina bodies were identified, and brainstem motor nuclei and motor cortex were normal. As such, the clinical and pathologic findings argue against comorbid, clinically unrecognized ALS and next-generation sequencing did not reveal a pathogenetic mutation (e.g. *VCP*, *SQSTM1*, *TARDBP*, *FUS*, and *HNRNPA1*) as seen in multisystem proteinopathies. The finding of mild motor neuron pathology in sIBM is intriguing and is consistent with earlier evidence for a neurogenic component in the disease. This raises the question of whether sIBM patients can have a secondary motor neuron injury following their peripherally located primary insult that involves muscle, neuromuscular junction, and/or distal

axon. Additional postmortem studies are needed to better understand the role of spinal cord and axonal pathologies in sIBM.

REFERENCES

1. Askanas V, Engel WK. Inclusion-body myositis, a multifactorial muscle disease associated with aging: current concepts of pathogenesis. Curr Opin Rheumatol 2007;19:550–9
2. Brady S, Squier W, Sewry C, et al. A retrospective cohort study identifying the principal pathological features useful in the diagnosis of inclusion body myositis. BMJ Open 2014;4:e004552
3. Eisen A, Berry K, Gibson G. Inclusion body myositis (IBM): myopathy or neuropathy? Neurology 1983;33:1109–14
4. Lindberg C, Oldfors A, Hedstrom A. Inclusion body myositis: peripheral nerve involvement. Combined morphological and electrophysiological studies on peripheral nerves. J Neurol Sci 1990;99:327–38
5. Gonzalez-Perez P, Cirulli ET, Drory VE, et al. Novel mutation in VCP gene causes atypical amyotrophic lateral sclerosis. Neurology 2012;79:2201–8
6. Rossor AM, Jaunmuktane Z, Rossor MN, et al. TDP43 pathology in the brain, spinal cord, and dorsal root ganglia of a patient with FOSMN. Neurology 2019;92:e951–e6
7. Suzuki Y, Aizawa H, Sakashita K, et al. Autopsy-proven case of paraneoplastic lower motor neuron disease with sensorimotor neuropathy due to Waldenstrom's macroglobulinemia. Neuropathology 2018;38:568–73
8. Martinez-Lage M, Molina-Porcel L, Falcone D, et al. TDP-43 pathology in a case of hereditary spastic paraplegia with a NIPA1/SPG6 mutation. Acta Neuropathol 2012;124:285–91
9. Tan CF, Yamada M, Toyoshima Y, et al. Selective occurrence of TDP-43-immunoreactive inclusions in the lower motor neurons in Machado-Joseph disease. Acta Neuropathol 2009;118:553–60